



Research article

Estimation of global soil respiration by accounting for land-use changes derived from remote sensing data



Minaco Adachi ^{a, d,*}, Akihiko Ito ^b, Seiichiro Yonemura ^c, Wataru Takeuchi ^a

^a Institute of Industrial Science, The University of Tokyo, 4-6-1 Komaba, Meguro-ku, Tokyo, 153-8505, Japan

^b National Institute for Environmental Studies, 16-2 Onogawa, Tsukuba, Ibaraki, 305-8506, Japan

^c National Institute for Agro-Environmental Studies, NARO, 3-1-3 Kannondai, Tsukuba, Ibaraki, 305-8604, Japan

^d Graduate School of Life and Environmental Science, The University of Tsukuba, 1-1-1 Tennodai, Tsukuba, Ibaraki, 305-8577, Japan

ARTICLE INFO

Article history:

Received 25 November 2016

Received in revised form

24 May 2017

Accepted 25 May 2017

Keywords:

Soil temperature

MODIS

Land-use change

ABSTRACT

Soil respiration is one of the largest carbon fluxes from terrestrial ecosystems. Estimating global soil respiration is difficult because of its high spatiotemporal variability and sensitivity to land-use change. Satellite monitoring provides useful data for estimating the global carbon budget, but few studies have estimated global soil respiration using satellite data. We provide preliminary insights into the estimation of global soil respiration in 2001 and 2009 using empirically derived soil temperature equations for 17 ecosystems obtained by field studies, as well as MODIS climate data and land-use maps at a 4-km resolution. The daytime surface temperature from winter to early summer based on the MODIS data tended to be higher than the field-observed soil temperatures in subarctic and temperate ecosystems. The estimated global soil respiration was 94.8 and 93.8 Pg C yr⁻¹ in 2001 and 2009, respectively. However, the MODIS land-use maps had insufficient spatial resolution to evaluate the effect of land-use change on soil respiration. The spatial variation of soil respiration (Q_{10}) values was higher but its spatial variation was lower in high-latitude areas than in other areas. However, Q_{10} in tropical areas was more variable and was not accurately estimated (the values were >7.5 or <1.0) because of the low seasonal variation in soil respiration in tropical ecosystems. To solve these problems, it will be necessary to validate our results using a combination of remote sensing data at higher spatial resolution and field observations for many different ecosystems, and it will be necessary to account for the effects of more soil factors in the predictive equations.

© 2017 Elsevier Ltd. All rights reserved.

1. Introduction

Soil is a major carbon (C) reserve in terrestrial ecosystems. Soil respiration (R_s) is a large carbon flux from terrestrial ecosystems to the atmosphere. R_s is related to the amount of soil carbon input, soil carbon stocks, root biomass, microbial biomass, temperature, and soil water content (Davidson and Janssens, 2006; Sato et al., 2015). Soil organic carbon (SOC) dynamics at global scales, which include R_s , have many uncertainties, and the estimation of global R_s is difficult because of high spatiotemporal variability (Smith and Fang, 2010). As a result, estimates of global R_s have varied widely, ranging

from 68 PgC yr⁻¹ (Raich and Schlesinger, 1992) to 98 PgC yr⁻¹ (Bond-Lamberty and Thomson, 2010). Soil temperature is the main factor that influences soil carbon dynamics (Carvalhais et al., 2014; Davidson and Janssens, 2006), including R_s (Bond-Lamberty and Thomson, 2010; Raich and Schlesinger, 1992; Reichstein and Beer, 2008; Zhou et al., 2009). In one study, the temperature sensitivity of R_s per 10 °C change in temperature (i.e., Q_{10}) at a global scale varied from 1.43 to 2.03 among ecosystems (Zhou et al., 2009), but in another, the mean global Q_{10} was lower, at 1.4 (Hashimoto et al., 2015). In other cases, low soil water content decreased R_s of a savanna landscape under extremely dry conditions (Chen et al., 2002), whereas a decrease in the depth to ground water decreased R_s in a tropical swamp forest (Hirano et al., 2014). As a result, some models of R_s also include a soil moisture term (e.g., Sotta et al., 2004).

Land-use change also affects the SOC content since the accumulation rates of soil carbon change in response to changes in the

* Corresponding author. Graduate school of Life and Environmental Science, The University of Tsukuba, 1-1-1 Tennodai, Tsukuba, Ibaraki, 305-8577, Japan. Tel & Fax : +81-29-853-8857

E-mail addresses: adachi.minaco.gf@u.tsukuba.ac.jp (M. Adachi), [\(A. Ito\)](mailto:ito@nies.go.jp), yone@affrc.go.jp (S. Yonemura), wataru@iis.u-tokyo.ac.jp (W. Takeuchi).

input rates of organic matter, in decomposition rates, and in physical and biological conditions in the soil that result from land-use changes (Post and Kwon, 2000). According to a meta-analysis by Guo and Gifford (2002), the conversion of natural forest or pasture into cropland decreases soil carbon stocks. Therefore, estimates of global R_s should account for changes in land use and the differences in R_s among ecosystem types.

Satellite monitoring provides not only land cover maps but also useful vegetation and environmental data that can be used to estimate the global carbon budget in terrestrial ecosystems, and especially the carbon exchange between the atmosphere and ecosystems, because it permits estimates of the land surface temperature, gross primary production (GPP), net primary production (NPP), and leaf area index (Guo et al., 2012). For instance, these datasets from the Moderate Resolution Imaging Spectroradiometer (MODIS) have been used as inputs for carbon cycling models (e.g., Ise et al., 2010; Sasai et al., 2005, 2011; Yuan et al., 2015).

It is important to understand both the overall CO₂ budget of terrestrial ecosystems and the CO₂ dynamics in each compartment (e.g., plants versus soil). Although remote sensing cannot directly observe R_s , long-term and global R_s can be estimated based on the values of environmental factors (such as surface temperatures) that control R_s and that can be observed by remote sensing. Estimates of global R_s will provide accuracy comparable to that of other satellite data (e.g., data from the Greenhouse gases observing satellite; Yokota et al., 2009) and can be used to improve our understanding of the sources of changes in carbon cycling from ecosystems. However, no studies have evaluated the effect of land-use change on global R_s using MODIS remote sensing data.

In the present study, we provide preliminary insights into the estimation of global R_s by combining empirical equations derived from field studies with satellite data (climate and land cover). Our objectives were to (1) obtain soil temperature data using MODIS land surface temperature data, (2) identify the variation in global R_s and Q₁₀ from 2001 to 2009, and (3) discuss the effects of land-use change on global R_s .

2. Materials and methods

2.1. MODIS data

Daily MODIS land surface temperatures during the day and night (LST_d and LST_n, respectively) were calculated by interpolation using some remote sensing data (e.g., the 8-day composite LST at a 4-km spatial resolution from the MOD11C3, and vegetation data at a 10-m resolution from the AVNIR2). This approach was necessary because data with high spatial resolution may not cover sufficiently large areas for a given study (Takeuchi et al., 2012), as was the case in the present global-scale study. When vegetation was present, LST_d and LST_n were estimated above the vegetation. Soil water content (SWC) was estimated using the modified Keetch-Byram drought index (KBDI) based on remote sensing data (Keetch and Byram, 1968; Takeuchi et al., 2010), as follows:

$$\text{SWC} = \text{SWC}_{\max} [1 - (\text{KBDI} / 800)] \quad (1)$$

where SWC_{max} is the maximum soil water content at each study site based on published data, but most R_s equations do not include SWC parameters (summarized in Table S1 of the supporting information). Land cover was distinguished for the 17 ecosystem types in the table using the MODIS MOD12Q1 (collection 5) at a 4-km spatial resolution. This classification scheme was developed by the International Geosphere–Biosphere Programme Data and

Information Systems initiative (Friedl et al., 2002). This land cover map did not detect the paddy field and tundra classes. Each point in the land cover map from the MOD12Q1 was assigned to one of the 17 ecosystem classes.

2.2. Validation of MODIS surface temperatures using field observation

R_s in this study was predominantly estimated as a function of soil temperature (Table S1). We compared the MODIS estimates (LST_d and LST_n) to empirical data based on field observations (daily mean air temperature and soil temperature) at five sites: an evergreen needleleaf forest in Alaska (64°52'N, 147°51'W; Ueyama et al., 2014), a mixed forest in Japan (36°08'N, 137°25'E; from the AsiaFlux database, <http://asiaflux.net>), cropland in Japan (36°01'N, 140°07'E; Kishimoto-Mo et al., unpublished data), an evergreen broadleaf forest in Thailand (14°29'N, 101°54'E, AsiaFlux database), and an evergreen broadleaf forest in Malaysia (2°58'N, 102°18'E, AsiaFlux database). The measurement height for air temperature and the depth of the soil temperature measurement differed among the five sites, with respective values of 800 cm and –10 cm in the evergreen needleleaf forest, 1800 cm and –1 cm in the mixed forest, 200 cm and –2 cm in the cropland, 4500 cm and –5 cm in the evergreen broadleaf forest in Thailand, and 5300 cm and –2 cm in the evergreen broadleaf forest in Malaysia. We could not quantify the effects of these different measurement heights on estimation of R_s in each ecosystem because LST_d and LST_n were measured at the top of the dominant vegetation, and that height varied with the type of vegetation.

Table S1 provides the empirical equations for estimating R_s in the 17 ecosystems from around the world. We selected empirical equations that were based on field measurements (not data obtained using incubation or manipulation experiments) conducted since 2000 from version 3.0 of a global R_s database (Bond-Lamberty and Thomson, 2014). Daily R_s values were estimated using the empirical R_s equation corresponding to the land use type for each pixel, the estimated soil temperature, and the soil water content in each pixel of the grid (Fig. 1). R_s in the evergreen broadleaf forest, which is mainly a tropical forest, was estimated using only the soil water content when land surface temperature (LST) was >25 °C (Sotta et al., 2004). In addition, LST of grassland vegetation areas were sometimes more than 30 °C, and if we calculated R_s using an exponential function, the estimated R_s was unrealistically high in these areas. Richards et al. (2012) reported that R_s in a savanna decreased when the soil temperature was over 30 °C. Thus, if the LST for a savanna pixel was >30 °C, we recalculated LST to be less than 26 °C for the estimation of R_s in the ecosystems that included savanna vegetation (closed and open shrubland, grassland, savanna, woody savanna, grassland, cropland, and cropland–natural vegetation mosaic).

We modelled the dependency of R_s on temperature at a global scale according to the following relationship:

$$R_{s_est} = \alpha \times e^{\beta T} \quad (2)$$

where R_{s_est} is the estimated daily R_s in this study, T is the LST_d at each point (4-km resolution), and α and β are fitting parameters. We calculated R_{s_est} using the least-squares method based on R_s (Table S1) and LST_d over 365 days at a 4-km resolution. We calculated the Q₁₀ of R_s as follows:

$$Q_{10} = e^{10\beta} \quad (3)$$

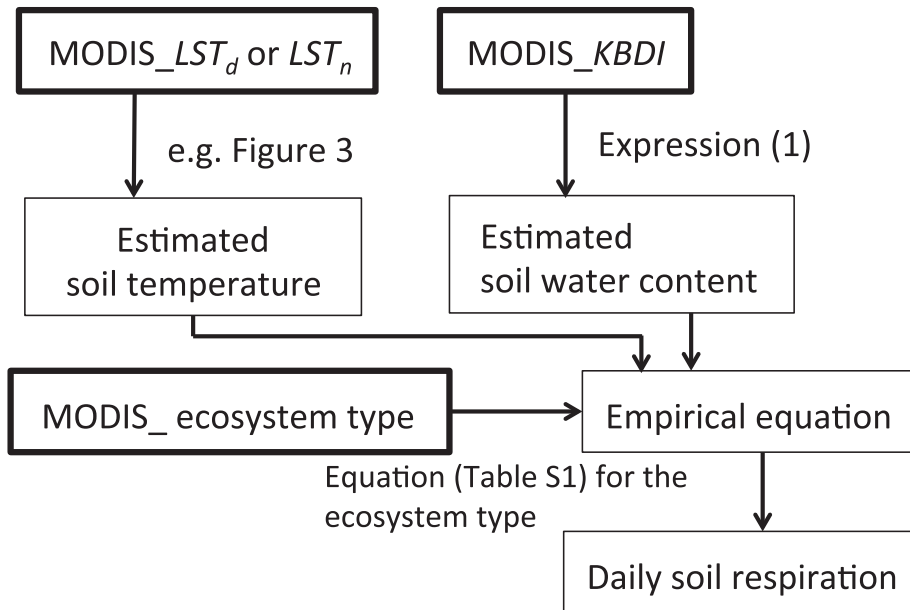


Fig. 1. An overview of the estimation process for daily soil respiration at a global scale. KBDI, Keetch–Byram drought index.

2.3. Statistical analyses

Statistical analyses were performed using version 3.3.1 of the R software (R Development Core Team, 2016). Pearson's product-moment correlation coefficient was used to clarify relations between LST_n values and soil temperature based on field data from the evergreen needleleaf forest, mixed forest, and cropland areas (Fig. 3).

3. Results

3.1. Estimation of soil temperature

We compared LST_d and LST_n in the five ecosystems with the observed daily mean air and soil temperatures in the field (Fig. 2). At the Alaska and Japan sites, the observed soil temperatures from winter to early summer were lower than the LST_d (Fig. 2a–c). LST_n values in these ecosystems were significantly correlated with the soil temperature from winter to early summer (Fig. 3, $P < 0.001$). We estimated soil temperatures during the winter to early summer for subarctic and temperate areas using the equations in Fig. 3, which used LST_n to calculate R_s in six of the ecosystems: evergreen needleleaf forest, deciduous needleleaf forest, deciduous broadleaf forest, mixed forest, cropland, and the cropland–natural vegetation mosaic. In the tropical regions, LST_d was generally lower than the actual air temperature in the evergreen broadleaf forests in Thailand (Fig. 2d).

3.2. Land-use change

To quantify the magnitude of land-use change, we counted the number of pixels for each ecosystem type based on the MODIS land cover maps in 2001 and 2009 and used these sums to calculate the percentage of the total area occupied by each ecosystem (Table S2). The cropland and cropland–natural vegetation mosaic types accounted for approximately 10% of the world's land area in both years, but the cropland–natural vegetation mosaic decreased from 4.0% of the total land area in 2001 to 3.6% in 2009. The total forest area (evergreen needleleaf forest, evergreen broadleaf forest,

deciduous needleleaf forest, deciduous broadleaf forest, and mixed forest) increased from 14.1% in 2001 to 15.3% in 2009. In particular, the areas of evergreen needleleaf forests in North America and Russia and of the deciduous needleleaf forest in northern Russia increased. The areas of grassland and woody savanna both decreased from 2001 to 2009.

3.3. Estimation of global R_s and Q_{10}

We estimated annual global R_s values of 94.8 and 93.8 Pg C yr⁻¹ in 2001 and 2009, respectively; Fig. 4 shows the regional distribution of the components of these total values. The mean annual R_s in each ecosystem except urban and built-up land, snow and ice, and tundra (for which R_s was assumed to equal 0) ranged from 77 to 1030 gC m⁻² yr⁻¹ in 2001 (Fig. 5). The decrease in global annual R_s from 2001 to 2009 was mainly caused by decreases in the areas of woody savanna, deciduous broadleaf forest, and the cropland–natural vegetation mosaic (Table S2). The spatial variation of the Q_{10} values was higher but its spatial variation was lower in high-latitude areas than in other areas (Fig. 6). However, Q_{10} values in tropical areas could not be accurately estimated (the values were >7.5 or <1.0) because of low seasonal variation in R_s in the tropical ecosystems (mainly evergreen broadleaf forest, savanna, and woody savanna). In addition, areas with low Q_{10} values in North America and Eurasia were mainly urban and built-up areas.

4. Discussion

Both the LST_d and the LST_n values based on MODIS data for the three ecosystems with field-observed temperature data were correlated with the observed daily mean air and soil temperatures, especially for the relationship between LST_n and soil temperature from winter to early summer in the subarctic and temperate ecosystems (Fig. 3). On the other hand, LST_d became similar to the autumn air and soil temperatures in the field for the evergreen needleleaf forest and mixed forest (Fig. 2a and b). These relationships would be influenced by two important aspects of plant phenology: leaf flushing and litterfall. Satellite data are often used to monitor plant phenology (Linderholm, 2006), and a combined

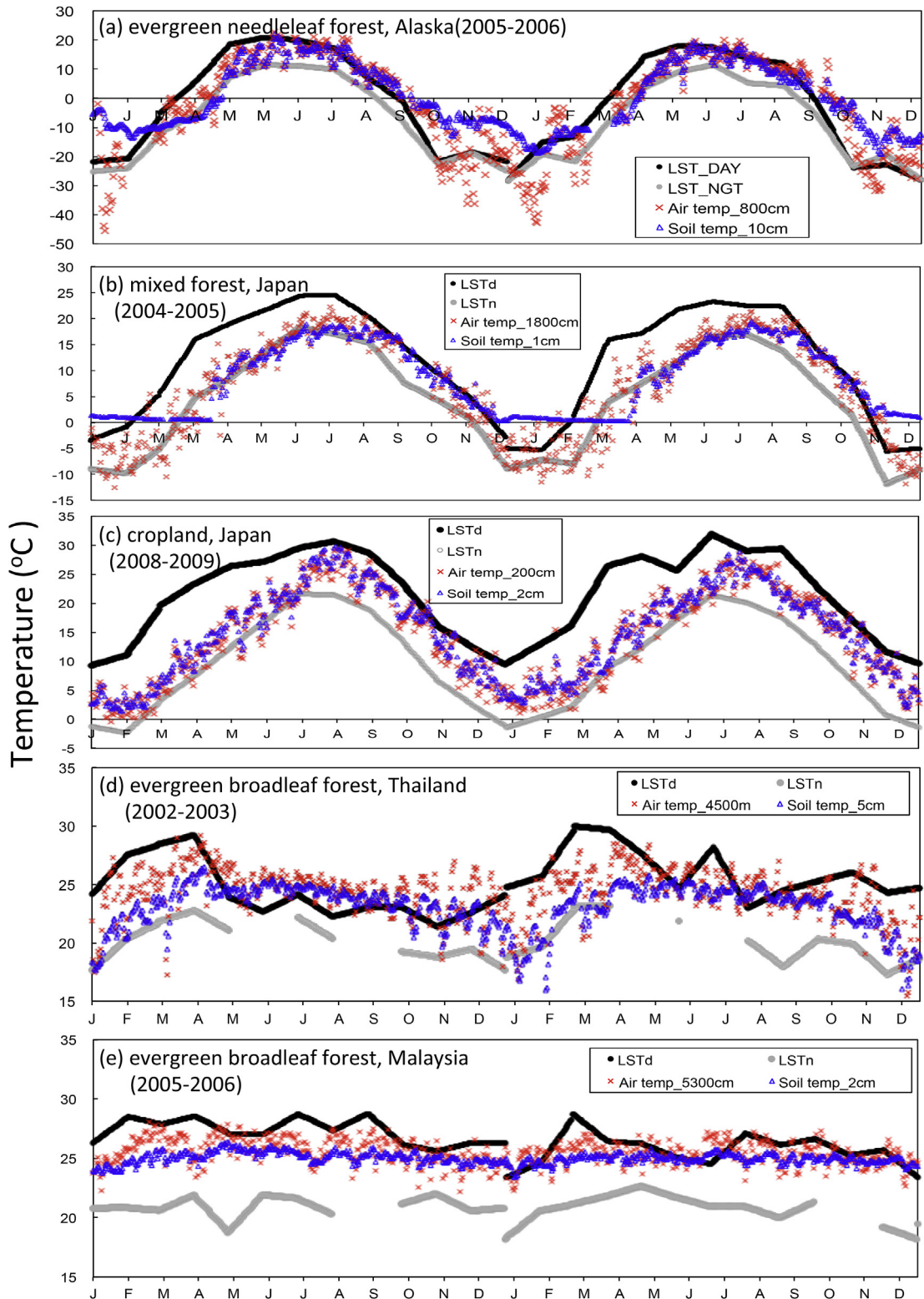


Fig. 2. Comparison between MODIS daytime and night surface temperatures (LST_d and LST_n), air temperature, and soil temperature and field observations in (a) an evergreen needleleaf forest in Alaska, (b) a mixed forest in Japan, (c) cropland in Japan, (d) an evergreen broadleaf forest in Thailand, and (e) an evergreen broadleaf forest in Malaysia. The observation period and heights of air and soil temperatures differed among the sites.

analysis of satellite and eddy-covariance data showed that environmental conditions influenced the annual trends in GPP (Xia et al., 2015). Mao et al. (2012) reported that the mean global GPP based on MODIS data was 111.58 PgC from 2000 to 2009, but they

did not report seasonal trends, unlike in the present study. Beer et al. (2010) reported that global GPP was approximately 123 Pg C yr^{-1} based on their observations (eddy-covariance flux data and models). However, the relationships between R_s and GPP are not

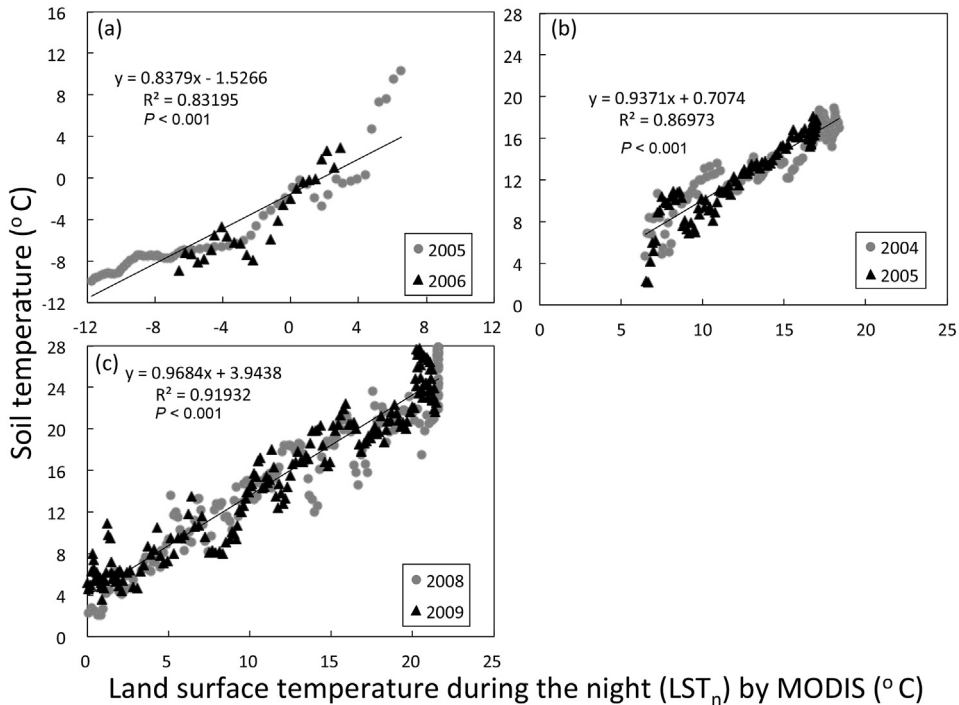


Fig. 3. The relationships between land surface temperature during the night (LST_n) based on the MODIS dataset and soil temperature based on observation data from (a) an evergreen needleleaf forest in Alaska (from March to April, $LST_n > -12.0^\circ\text{C}$), (b) a mixed forest in Japan (from April to July, $LST_n > 6.5^\circ\text{C}$) and (c) cropland in Japan (from January to July, $LST_n > 0.0^\circ\text{C}$).

clear at an ecosystem scale, so we must integrate and compare these components of the global terrestrial carbon cycle to more accurately characterize the response of R_s to climate change and land use change.

The global R_s in the present study that we estimated using MODIS data at a 4-km resolution was similar to the results that have been estimated using field observation data: 98 Pg C yr⁻¹ in 2008 (Bond-Lamberty and Thomson, 2010), and 93.2 Pg C yr⁻¹ in 2001 and 92.7 Pg C yr⁻¹ in 2009 (Hashimoto et al., 2015). Some studies have reported that global R_s in the 2000s was greater than the values in the 1980s and 1990s (Bond-Lamberty and Thomson, 2010; Hashimoto et al., 2015). In the present study, the mean annual R_s values for each ecosystem did not differ between 2001 and 2009 (Fig. 5). Because of a hiatus in global warming, the average global annual temperature did not rise greatly between 1998 and 2012 (Kaufmann et al., 2011; Kosaka and Xie, 2013). On the other hand, our estimates of R_s did not show high spatial variation, even though field observations indicated high spatial variation; for example, the annual R_s in temperate grassland ranged from 32 to 2800 gC m⁻² yr⁻¹ (Bond-Lamberty and Thomson, 2014). Bond-Lamberty and Thomson (2010) showed that the annual R_s based on field observations had high variation because the annual R_s of some temperate and tropical biomes were greater than 2000 gC m⁻² yr⁻¹. We found higher spatial variation of the Q_{10} values in high-latitude areas than in other areas, but its spatial variation was lower and we could not reliably estimate Q_{10} values in the tropical areas (Fig. 6). Zhou et al. (2009) reported that Q_{10} values were highest in tundra regions (2.03), whereas the Q_{10} of evergreen broadleaf forest (mainly in tropical regions) was only 1.50. Hashimoto et al. (2015) also estimated that Q_{10} values in tropical regions were less than 1.5. Our results suggested that LST_d in evergreen broadleaf forest showed low temporal variation (Fig. 2e), and this would be one reason for uncertainty in the estimation of Q_{10} values in the tropical areas.

We estimated the annual R_s using one empirical equation for each ecosystem; however, it is unlikely that these equations remain sufficiently representative over large areas. To solve this issue, we need to validate the annual R_s and empirical equations using field observations from many different ecosystems. Moreover, we did not validate soil water content using field observation data because we relied on previously published equations for R_s for all ecosystems, and most of the equations did not include soil water content as a regression parameter. Some papers did not measure R_s during the winter or snowy season; for example, this was true for evergreen broadleaf forest (Pypker and Fredeen, 2002) and larch forest (Jiang et al., 2005). Mo et al. (2005) suggested that R_s measured above a snow surface accounted for approximately 6–10% of the annual R_s in a cool temperate forest. Therefore, differences in the measurement period used to develop the empirical equations in Table S1 increased the uncertainty of our estimation of global R_s . Additionally, some studies reported that annual R_s changed in response to the age of vegetation (Sauvage et al., 2006) and soil texture: clayey and sandy soils (Sugihara et al., 2012) and different management regimes (Richards et al., 2012; Yonemura et al., 2014) produced different results under the same climatic conditions. Janssens et al. (2010) reported an increase in nitrogen deposition from combustion of fossil fuels, and that this fertilization decreased R_s . However, elevated atmospheric CO₂ increased soil microbial activity and decomposition of soil organic matter, which would increase R_s (Carney et al., 2007). Therefore, we need to consider these factors (e.g., the effect of land-use change, age of vegetation, soil texture, SOC, and nitrogen fertilization) when estimating R_s and validate our results using field observations.

The global R_s in the present study decreased by 1.0 Pg C yr⁻¹ from 2001 to 2009, but we did not consider the net effect on the carbon flux due to the observed land-use changes. Houghton et al. (2012) estimated that the mean net carbon flux from land-use

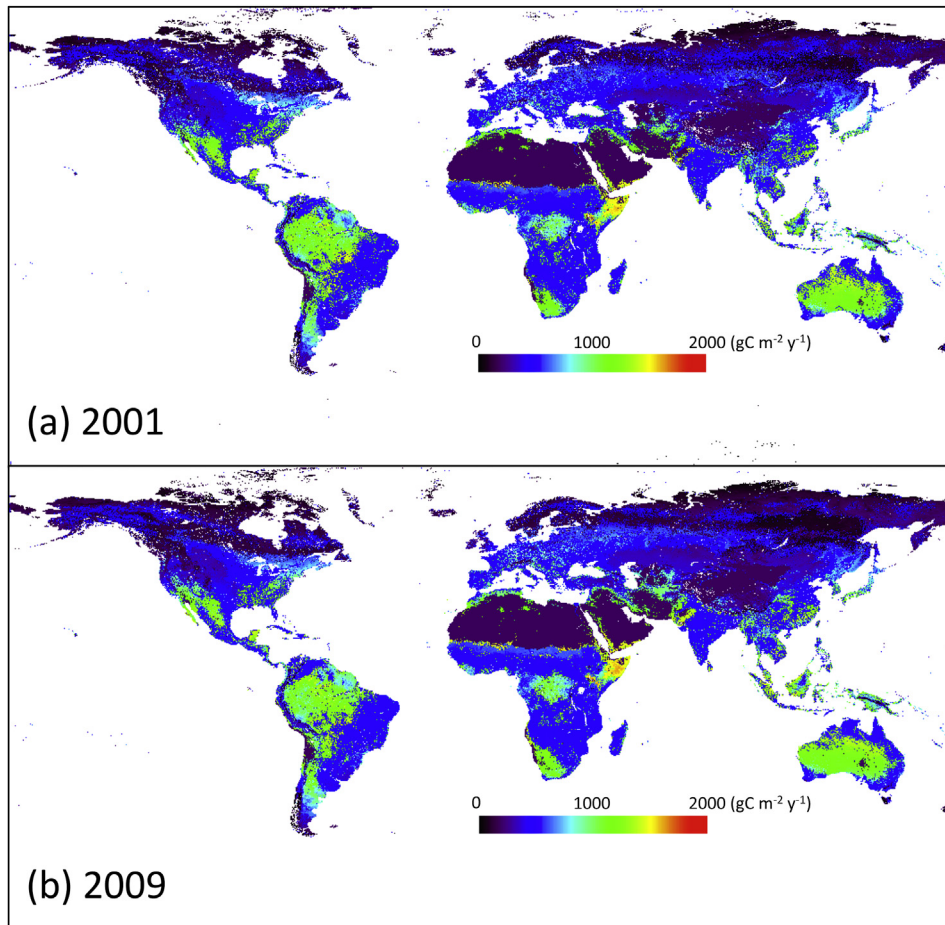


Fig. 4. Map of the global distribution of total annual soil respiration (R_s) in (a) 2001 and (b) 2009.

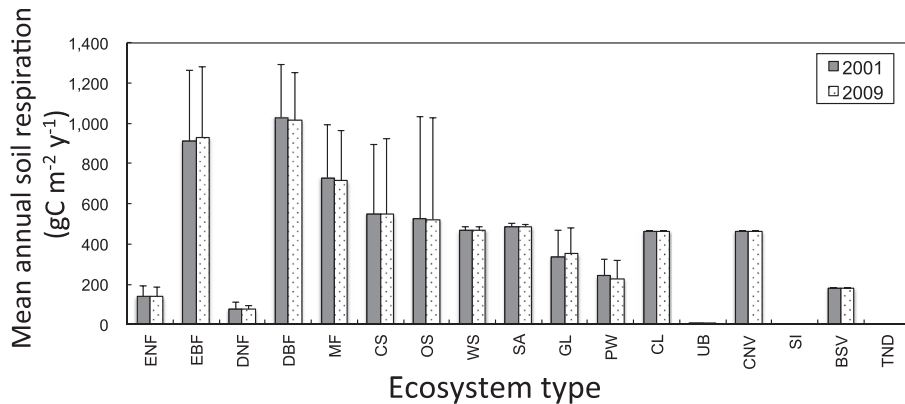


Fig. 5. Mean annual soil respiration (R_s) in the 17 ecosystems in 2001 and 2009. Table S1 presents the R_s equations for each ecosystem type. Values are means \pm standard deviations. None of the differences between 2001 and 2009 were statistically significant. ENF, evergreen needleleaf forest; EBF, evergreen broadleaf forest; DNF, deciduous needleleaf forest; DBF, deciduous broadleaf forest; MF, mixed forest; CS, closed shrublands; OS, open shrubland; WS, woody savanna; SA, savanna; GL, grassland; PW, permanent wetland; CL, cropland; UB, urban and build-up; CNV, cropland/natural vegetation mosaic; SI, snow and ice; BSV, barren or sparsely vegetated; TND, tundra.

change from 2000 to 2009 was a decrease of 1.1 Pg C yr^{-1} , and $0.12 \text{ Pg C yr}^{-1}$ of this (about 10%) was due to forest degradation. The annual global SR in 2009 decreased by 1.0 Pg C yr^{-1} (from that in 2001, mainly due to decreased areas of woody savanna, deciduous broadleaf forest and the cropland–natural vegetation mosaic. However, the previously reported decrease in the area of evergreen broadleaf forest (mainly in tropical regions; Hansen et al., 2010;

Keenan et al., 2015) could not be detected in the MODIS land cover map in the present study. In addition, woody savanna and savanna were difficult to distinguish based on the MODIS data. We therefore need to do more work to develop MODIS products, and especially global land cover maps, at high spatial resolution that will let us better detect land-use changes and evaluate the effects of these changes on the global carbon cycle.

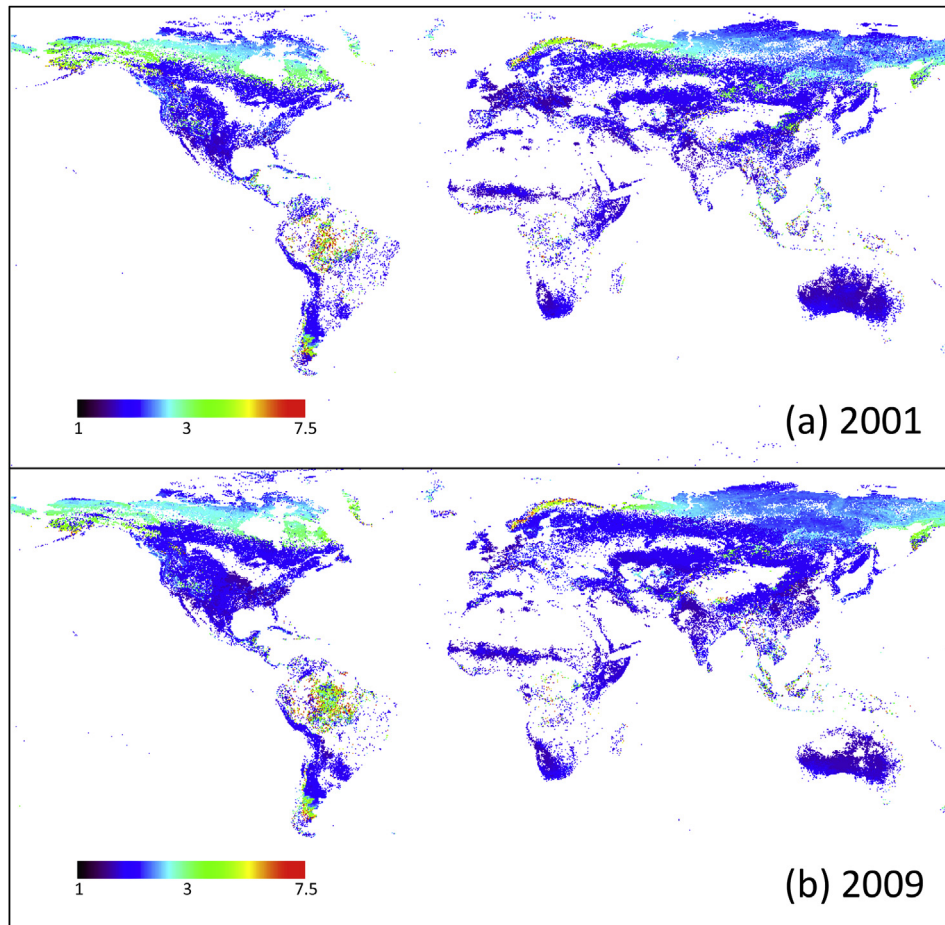


Fig. 6. Spatial variation in Q_{10} values estimated using the daily soil respiration (R_s) values and MODIS land surface temperatures during the daytime (LST_d).

5. Conclusions

In the present study, we provided preliminary insights into the estimation of global R_s in 2001 and 2009 using empirically derived soil temperature equations for 17 ecosystems, climate data, and 4-km-resolution MODIS land-use maps. Land surface temperatures during the night (LST_n) in the MODIS dataset were also important to estimate global R_s as were daytime LST values (LST_d) from winter to early summer in subarctic and temperate ecosystems. The annual global R_s values did not differ greatly between 2001 and 2009 (94.8 and 93.8 Pg C yr $^{-1}$, respectively), but did suggest a slight decrease. The decrease in annual global R_s in 2009 resulted mainly from decreased areas of woody savanna, deciduous broadleaf forest, and the cropland–natural vegetation mosaic. However, due to the high uncertainties in the input data and equations used in our analysis, it will be necessary to develop more accurate estimates of global R_s by (1) considering other factors that affect R_s (e.g., age of vegetation, soil texture, SOC, and nitrogen fertilization) and (2) using global climate data and land-use maps obtained at higher spatial resolution.

Acknowledgements

This research was supported by Green Network of Excellence project (GRENE-ei; <http://grene.jp/english/>) and by the Ministry of Education, Culture, Sports, Science and Technology, Japan. This research was also supported by JSPS KAKENHI Grant Number 16H05787. We thank Dr A.W. Kishimoto-Mo of the National

Institute for Agro-Environmental Studies for providing the climate data from Tsukuba, Japan, and Dr M. Ueyama of Osaka Prefecture University, Dr H. Iwata of Shinshu University, and Dr Y. Harazono of the International Arctic Research Center, University of Alaska at Fairbanks, for providing the climate data from Alaska. We also thank Dr T. Maeda of the National Institute of Advanced Industrial Science and Technology, Dr Y. Kosugi of Kyoto University, and the researchers responsible for the AsiaFlux Database (<http://asiaflux.net>) for providing the climate data from Takayama (Japan), Sakaerat (Thailand), and Pasoh (Malaysia).

Appendix A. Supplementary data

Supplementary data related to this article can be found at <http://dx.doi.org/10.1016/j.jenvman.2017.05.076>.

References

- Beer, C., Reichstein, M., Tomelleri, E., Ciais, P., Jung, M., Carvalhais, N., Rödenbeck, C., Arain, M.A., Baldocchi, D., Bonan, G.B., Bondeau, A., Cescatti, A., Lasslop, G., Lindroth, A., Lomas, M., Luysaert, S., Margolis, H., Oleson, K.W., Roupsard, O., Veenendaal, E., Viovy, N., Williams, C., Woodward, F.I., Papale, D., 2010. Terrestrial gross carbon dioxide uptake: global distribution and covariation with climate. *Science* 329, 834–838.
- Bond-Lamberty, B.P., Thomson, A.M., 2010. Temperature-associated increases in the global soil respiration record. *Nature* 464, 579–583.
- Bond-Lamberty, B.P., Thomson, A.M., 2014. A Global Database of Soil Respiration Data, Version 3.0. Data set, Available on-line from Oak Ridge National Laboratory Distributed Active Archive Center, Oak Ridge, Tennessee, USA. <http://daac.ornl.gov> (Accessed 16 September 2016).
- Carney, K.M., Hungate, B.A., Drake, B.G., Megonigal, J.P., 2007. Altered soil microbial

- community at elevated CO₂ leads to loss of soil carbon. *P. Natl. Acad. Sci.* 104, 4990–4995.
- Carvalhais, N., Forkel, M., Khomik, M., Bellarby, J., Jung, M., Migliavacca, M., Mu, M., Saatchi, S., Santoro, M., Thurner, M., Weber, U., Ahrens, B., Beer, C., Cescatti, A., Randerson, J.T., Reichstein, M., 2014. Global covariation of carbon turnover times with climate in terrestrial ecosystems. *Nature* 514, 213–217.
- Chen, X., Eamus, D., Hutley, L.B., 2002. Seasonal patterns of soil carbon dioxide efflux from a wet-dry tropical savanna of northern Australia. *Aust. J. Bot.* 50, 43–51.
- Davidson, E.A., Janssens, I.A., 2006. Temperature sensitivity of soil carbon decomposition and feedbacks to climate change. *Nature* 440, 165–173.
- Friedl, M.A., McIver, D.K., Hodges, J.C.F., Zhang, X.Y., Muchoney, D., Strahler, A.H., Woodcock, C.E., Gopal, S., Schneider, A., Cooper, A., Baccini, A., Gao, F., Schaaf, C., 2002. Global land cover mapping from MODIS: algorithms and early results. *Remote Sens. Environ.* 83, 287–302.
- Guo, L.B., Gifford, R.M., 2002. Soil carbon stocks and land use change: a meta analysis. *Glob. Change Biol.* 8, 345–360.
- Guo, M., Wang, X., Li, J., Yi, K., Zhong, G., Tani, H., 2012. Assessment of global carbon dioxide concentration using MODIS and GOSAT data. *Sensors* 12, 16368–16389.
- Hansen, M.C., Stehman, S.V., Potapov, P.V., 2010. Quantification of global gross forest cover loss. *P. Natl. Acad. Sci.* 107, 8650–8655. <http://dx.doi.org/10.1073/pnas.0912668107>.
- Hashimoto, S., Carvalhais, N., Ito, A., Migliavacca, M., Nishina, K., Reichstein, M., 2015. Global spatiotemporal distribution of soil respiration modeled using a global database. *Biogeosciences* 12, 4121–4132.
- Hirano, T., Kusin, K., Limin, S., Osaki, M., 2014. Carbon dioxide emissions through oxidative peat decomposition on a burnt tropical peatland. *Glob. Change Biol.* 20, 555–565.
- Houghton, R.A., House, J.I., Pongratz, J., van der Werf, G.R., DeFries, R.S., Hansen, M.C., Le Quéré, Ramankutty, N., 2012. Carbon emissions from land use and land-cover change. *Biogeosciences* 9, 5125–5142.
- Ise, T., Litton, C.M., Giardina, C.P., Ito, A., 2010. Comparison of modeling approaches for carbon partitioning: impact on estimates of global net primary production and equilibrium biomass of woody vegetation from MODIS GPP. *J. Geophys. Res.* 115, G04025.
- Janssens, I.A., Dieleman, W., Luyssaert, S., Subke, J.-A., Reichstein, M., Ceulemans, R., Ciais, P., Dolman, A.J., Grace, J., Matteucci, G., Papale, D., Piao, S.L., Schulze, E.-D., Tang, J., Law, B.E., 2010. Reduction of forest soil respiration in response to nitrogen deposition. *Nat. Geosci.* 3, 315–322.
- Jiang, L., Shi, F., Li, B., Luo, Y., Chen, J., Chen, J., 2005. Separating rhizosphere respiration from total soil respiration in two larch plantation in northeastern China. *Tree Physiol.* 25, 1187–1195.
- Kaufmann, R.K., Kauppi, H., Mann, M.L., Stock, J.H., 2011. Reconciling anthropogenic climate change with observed temperature 1998–2008. *P. Natl. Acad. Sci.* 108, 11790–11793.
- Keenan, R.J., Reams, G.A., Achard, F., de Freitas, J.V., Grainger, A., Lindquist, E., 2015. Dynamics of global forest area: results from the FAO global forest resources assessment 2015. *For. Ecol. Manag.* 352, 9–20.
- Keetch, J.J., Byram, G.M., 1968. A Drought Index for Forest Fire Control, Res. Paper SE-38. U.S. Department of Agriculture, Forest Service. Southeastern Forest Experiment Station, Asheville, NC.
- Kosaka, Y., Xie, S.-P., 2013. Recent global-warming hiatus tied to equatorial Pacific surface cooling. *Nature* 501, 403–407.
- Linderholm, H.W., 2006. Growing season changes in the last century. *Agr. For. Meteorol.* 137, 1–14.
- Mao, J., Thornton, P.E., Shi, X., Zhao, M., Post, W.M., 2012. Remote sensing evaluation of CLM4 GPP for the period 2000–09. *J. Clim.* 25, 5327–5342.
- Mo, W., Lee, M.S., Uchida, M., Inatomi, M., Saigusa, N., Mariko, S., Koizumi, H., 2005. Seasonal and annual variations in soil respiration in a cool-temperate deciduous broad-leaved forest in Japan. *Agr. For. Meteorol.* 134, 81–94.
- Post, W.M., Kwon, K.C., 2000. Soil carbon sequestration and land-use change: processes and potential. *Glob. Change Biol.* 6, 317–327.
- Pypker, T.G., Fredeen, A.L., 2002. Ecosystem CO₂ flux over two growing seasons for a sub-Boreal clearcut 5 and 6 years after harvest. *Agr. For. Meteorol.* 114, 15–30.
- Raich, J.W., Schelesinger, W.H., 1992. The global carbon dioxide flux in soil respiration and its relationship to vegetation and climate. *Tellus* 44B, 81–99.
- R Development Core Team: R, 2016. A Language and Environment for Statistical Computing. R Foundation for Statistical Computing, Vienna, Austria. ISBN 3-900051-07-0, available at: <http://www.R-project.org/>.
- Reichstein, M., Beer, C., 2008. Soil respiration across scales: the importance of a model-data integration framework for data interpretation. *J. Plant Nutr. Soil Sci.* 171, 344–354.
- Richards, A.E., Dathe, J., Cook, G.D., 2012. Fire interacts with season to influence soil respiration in tropical savannas. *Soil Biol. Biochem.* 53, 90–98.
- Sasai, T., Ichii, K., Yamaguchi, Y., Nemani, R., 2005. Simulating terrestrial carbon fluxes using the new biosphere model “biosphere model integrating eco-physiological and mechanistic approaches using satellite data” (BEAMS). *J. Geophys. Res.* 110, G02014.
- Sasai, T., Saigusa, N., Nasahara, K.N., Ito, A., Hashimoto, H., Nemani, R., Hirata, R., Ichii, K., Takagi, K., Saitoh, T.M., Ohta, T., Murakami, K., Yamaguchi, Y., Oikawa, T., 2011. Satellite-driven estimation of terrestrial carbon flux over far east Asia with 1-km grid resolution. *Remote Sens. Environ.* 115, 1758–1771.
- Sato, H., Ito, A., Ito, A., Ise, T., Kato, E., 2015. Current status and future of land surface models. *Soil Sci. Plant Nutr.* 61, 34–47.
- Saurette, D.D., Chang, S., Thomas, B.R., 2006. Some characteristics of soil respiration in hybrid poplar plantations in northern Alberta. *Can. J. Soil Sci.* 86, 257–268.
- Smith, P., Fang, C., 2010. A warm response by soils. *Nature* 464, 499–500.
- Sotta, E.D., Meir, P., Malhi, Y., Nobre, A.D., Hodnett, M., Grace, J., 2004. Soil CO₂ efflux in a tropical forest in the central Amazon. *Glob. Change Biol.* 10, 601–617.
- Sugihara, S., Funakawa, S., Kilasara, M., Kosaki, T., 2012. Effects of land management on CO₂ flux and soil C stock in two Tanzanian croplands with contrasting soil texture. *Soil Biol. Biochem.* 46, 1–9.
- Takeuchi, W., Hirano, T., Anggraini, N., Roswintiarti, O., 2010. Estimation of Ground Water Table at Forested Peatland in Kalimantan Using Drought Index towards Wildfire Control. 31st Asian conference on remote sensing (ACRS), Hanoi, Vietnam.
- Takeuchi, W., Oyoshi, K., Akatsuka, S., 2012. Super-resolution of MTSAT land surface temperature by blending MODIS and AVNIR2. *Asian J. Geoinformat.* 12 (2).
- Ueyama, M., Iwata, H., Harazono, Y., 2014. Autumn warming reduces the CO₂ sink of a black spruce forest in interior Alaska based on a nine-year eddy covariance measurement. *Glob. Change Biol.* 20, 1161–1173.
- Xia, J., Niu, S., Ciais, P., Janssens, I.A., Chen, J., Ammann, C., Arain, A., Blanken, P.D., Cescatti, A., Bonal, D., Buchmann, N., Curtis, P.S., Chen, S., Dong, J., Flanagan, L.B., Frankenberg, C., Georgiadis, T., Gough, C.M., Hui, D., Kiely, G., Li, J., Lund, M., Mgliulo, V., Marcolla, B., Lutz, M., Montagnani, L., Moors, E.J., Olesen, J.E., Piao, S., Raschi, A., Roupsard, O., Suyker, A.E., Urbaniak, M., Vaccari, F.P., Varlagin, A., Vesala, T., Wilkinson, M., Weng, E., Wohlfahrt, G., Yan, L., Luo, Y., 2015. Joint control of terrestrial gross primary productivity by plant phenology and physiology. *P. Natl. Acad. Sci.* 112, 2788–2793.
- Yokota, T., Yoshida, Y., Eguchi, N., Ota, Y., Tanaka, T., Watanabe, H., Maksyutov, S., 2009. Global concentrations of CO₂ and CH₄ retrieved from GOSAT: first preliminary results. *SOLA* 5, 160–163.
- Yonemura, S., Nouchi, I., Nishimura, S., Sakurai, G., Togami, K., Yagi, K., 2014. Soil respiration, N₂O and CH₄ emissions from an Andisol under conventional-tillage and no-tillage cultivation for 4 years. *Biol. Fert. Soils* 50, 63–74.
- Yuan, W., Cai, W., Nguy-Robertson, A.L., Fang, H., Suyker, A.E., Chen, Y., Dong, W., Liu, S., Zhang, H., 2015. Uncertainty in simulating gross primary production of cropland ecosystem from satellite-based models. *Agr. For. Meteorol.* 207, 48–57.
- Zhou, T., Shi, P., Hui, D., Luo, Y., 2009. Global pattern of temperature sensitivity of soil heterotrophic respiration (Q_{10}) and its implications for carbon-climate feedback. *J. Geophys. Res.* 114, G02016.